
Continuous Diffusion for Mixed-Type Tabular Data

Markus Mueller

Kathrin Gruber

Dennis Fok

Econometric Institute

Erasmus University Rotterdam

{mueller, gruber, dfok}@ese.eur.nl

Abstract

Score-based generative models (or diffusion models for short) have proven successful across many domains in generating text and image data. However, the consideration of mixed-type tabular data with this model family has fallen short so far. Existing research mainly combines different diffusion processes without explicitly accounting for the feature heterogeneity inherent to tabular data. In this paper, we combine score matching and score interpolation to ensure a common type of continuous noise distribution that affects both continuous and categorical features alike. Further, we investigate the impact of distinct noise schedules per feature or per data type. We allow for adaptive, learnable noise schedules to ensure optimally allocated model capacity and balanced generative capability. Results show that our model consistently outperforms state-of-the-art benchmark models and that accounting for heterogeneity within the noise schedule design boosts the sample quality.

1 Introduction

Score-based generative models [1], also termed diffusion models [2, 3], have shown remarkable potential for the generation of images [4, 5], videos [6], text [7–9], molecules [10], and many other highly complex data structures. Although their standard formulation only applies to continuous data, the framework has since been adapted to categorical data in various ways, including discrete diffusion processes [11, 12], diffusion in continuous embedding space [7, 8, 13, 14], and others [15–17]. However, adaptations to data of mixed-type, which includes both continuous and categorical features alike, progress slowly.

A crucial component in score-based generative models is the noise schedule [9, 18–21]. Typical noise schedule designs focus on learning the timesteps most important to obtaining high quality samples [22, 23], while others attempt to learn the optimal noise schedule [8, 18]. Existing approaches for mixed-type tabular data, either combine distinct diffusion processes for continuous and discrete features to derive a joint model [24, 25], or treat the one-hot encoded categorical features as continuous during training [26]. However, the inherently different diffusion processes make it difficult to optimally balance the noise schedules across features (and feature types), which negatively affects the model’s allocation capacity across timesteps. Moreover, non-continuous noise processes do not allow for state-of-the-art image domain techniques such as accelerated sampling [27] or classifier-free guidance [28].

Lastly, but most importantly, the features’ domain, nature and marginal distribution can vary significantly [29]. For instance, any two continuous features may be subject to different levels of discretization or different bounds, even after applying common data pre-processing techniques; and any two categorical features may differ in the number of categories, or one feature is much more imbalanced than the other. An effective modeling of the joint distribution should therefore warrant potentially different noise schedules per data or feature type.

In this paper, we investigate possibilities to account for the feature heterogeneity in mixed-type tabular data with score-based generative models. First, we combine *score matching* [30] with the recently proposed method of *score interpolation* [8] to derive a score-based model that uses a Gaussian diffusion process for both continuous and categorical features. This way, the different noise processes become directly comparable, easier to balance, and also enable the application of, for instance, classifier-free guidance, accelerated sampling, or other diffusion-based image domain advances, to mixed-type tabular data. Second, similar to the idea behind non-uniform diffusion [31], we additionally investigate the use of feature-specific noise schedules and distinct noise schedules per feature type. Lastly, we make all noise schedules adaptive such that we can directly take feature or type heterogeneity into account. This ensures a better allocation of the model’s capacity across features and timesteps during training and generation, and improves sample quality.

2 Score-based Generative Framework

First, we briefly explain the score-based frameworks for continuous and categorical data types. Afterwards, these are combined in a single diffusion model to learn the joint distribution of the data.

2.1 Continuous Features

Without loss of generality, let $\{\mathbf{x}_t\}_{t=0}^1$ be a diffusion process that gradually adds noise in (scaled) continuous time $t \in [0, 1]$ to a vector of continuous features $\mathbf{x}_0 \equiv \mathbf{x}_{\text{cont}} \in \mathbb{R}^{K_{\text{cont}}}$. The data sample distribution at time t , $p_t(\mathbf{x})$, evolves from the real data distribution, $p_0(\mathbf{x})$, to a terminal distribution, $p_1(\mathbf{x})$. Our goal is to learn the reverse process that allows us to go from noise $\mathbf{x}_1 \sim p_1(\mathbf{x})$ to a new data sample $\mathbf{x}_0^* \sim p_0(\mathbf{x})$.

The forward-pass of such a continuous-time diffusion process is formulated as the solution to a stochastic differential equation (SDE):

$$d\mathbf{x} = \mathbf{f}(\mathbf{x}, t)dt + g(t)d\mathbf{w}, \quad (1)$$

where $\mathbf{f}(\cdot, t) : \mathbb{R}^{K_{\text{cont}}} \rightarrow \mathbb{R}^{K_{\text{cont}}}$ is the drift coefficient, $g(\cdot) : \mathbb{R} \rightarrow \mathbb{R}$ is the diffusion coefficient, and \mathbf{w} is the Brownian motion [1]. The reversion of this diffusion process yields the trajectory of \mathbf{x} as t goes backwards in time from 1 to 0. This reverse-time process can be formulated as a probability flow ordinary differential equation (ODE):

$$d\mathbf{x} = \left[\mathbf{f}(\mathbf{x}, t) - \frac{1}{2}g(t)^2 \nabla_{\mathbf{x}} \log p_t(\mathbf{x}) \right] dt. \quad (2)$$

In Eq. (2), the only unknown is the score function $\nabla_{\mathbf{x}_t} \log p(\mathbf{x}_t)$. We approximate the score function with training a time-dependent score-based model $s_{\theta}(\mathbf{x}, t)$, parameterized by θ , via *score matching* [30]. The denoising *score matching* objective is

$$\min_{\theta} \mathbb{E}_t \left[\lambda(t) \mathbb{E}_{\mathbf{x}_0} \mathbb{E}_{\mathbf{x}_t | \mathbf{x}_0} \left[\|s_{\theta}(\mathbf{x}_t, t) - \nabla_{\mathbf{x}_t} \log p_{0t}(\mathbf{x}_t | \mathbf{x}_0)\|_2^2 \right] \right], \quad (3)$$

where $\lambda : [0, 1] \rightarrow \mathbb{R}_+$ is a positive weighting function for timesteps t , $t \sim \mathcal{U}_{[0,1]}$, and $p_{0t}(\mathbf{x}_t | \mathbf{x}_0)$ is the noise-inducing conditional distribution that adds noise to the ground-truth data [32].

In this paper, we use the EDM formulation [23], that is, $\mathbf{f}(\cdot, t) = \mathbf{0}$ and $g(t) = \sqrt{2\sigma_t}$ such that $p_{0t}(\mathbf{x}_t | \mathbf{x}_0) = \mathcal{N}(\mathbf{x}_t | \mathbf{x}_0, \sigma_t^2 I)$. We start the reverse process with sampling $\mathbf{x}_1 \sim p_1(\mathbf{x}) = \mathcal{N}(\mathbf{0}, \sigma_1^2 I)$ for σ_1^2 being sufficiently large and $\mathbb{E}[\mathbf{x}_0] = \mathbf{0}$. Then, we gradually guide the samples towards high density regions in the data space with the trained score model replacing the unknown, true score function. In practice, ODE or predictor-corrector samplers can be used for this iterative, denoising process [1].

2.2 Categorical Features

Since the score function for categorical features is undefined, the score-based generative framework cannot be directly applied. Therefore, we use *score interpolation* [8] to push the diffusion of categorical data into Euclidean embedding space. This allows us to impose the same type of noise distribution on both categorical and continuous features. Moreover, the model is able to fully take feature-specific uncertainty at intermediate timesteps into account, which improves the consistency of

the generated samples [8]. We will show that *score interpolation* also facilitates an efficient modeling of subtle dependencies across various data types.

Let $x_{\text{cat}}^{(j)} \in \{1, \dots, C_j\}$ be the j -th categorical feature with C_j possible classes. We can associate a distinct, trainable d -dimensional embedding vector $\mathbf{e}_i \in \mathbb{R}^d$ with each class $i = 1, \dots, C_j$. We denote the embedding vector corresponding to the ground truth class for a single feature as $\mathbf{x}_0 \in \{\mathbf{e}_1, \dots, \mathbf{e}_{C_j}\}$ and its noisy variant at time t as $\mathbf{x}_t \sim \mathcal{N}(\mathbf{x}_0, \sigma_t^2 I_d)$.

Given \mathbf{x}_t and t , the expectation $\mathbb{E}_{p(\mathbf{x}_0|\mathbf{x}_t,t)}[\nabla_{\mathbf{x}_t} \log p_{0t}(\mathbf{x}_t|\mathbf{x}_0)]$ is the minimizer of Eq. (3). Accordingly, we have

$$\mathbb{E}_{p(\mathbf{x}_0|\mathbf{x}_t,t)} \nabla_{\mathbf{x}_t} \log p(\mathbf{x}_t|\mathbf{x}_0) = \mathbb{E}_{p(\mathbf{x}_0|\mathbf{x}_t,t)} \frac{\mathbf{x}_0 - \mathbf{x}_t}{\sigma_t^2} = \frac{\mathbb{E}_{p(\mathbf{x}_0|\mathbf{x}_t,t)}[\mathbf{x}_0] - \mathbf{x}_t}{\sigma_t^2}. \quad (4)$$

Thus, we can train a model to estimate $p(\mathbf{x}_0|\mathbf{x}_t,t)$ and to obtain $\hat{\mathbf{x}}_0 = \mathbb{E}_{p(\mathbf{x}_0|\mathbf{x}_t,t)}[\mathbf{x}_0]$ as the weighted average over the C_j possible embedding vectors, in order to derive a score function estimate. Since $p(\mathbf{x}_0 = \mathbf{e}_i|\mathbf{x}_t,t) = p(x_{\text{cat}}^{(j)} = i|\mathbf{x}_t,t)$, an estimate of $p(\mathbf{x}_0|\mathbf{x}_t,t)$ can be obtained via a classifier that predicts C_j class probabilities for the j -th feature and is trained via cross-entropy loss. The same framework applies to all categorical features in the dataset.

We start the generative process for each categorical feature from an embedding vector $\mathbf{x}_1 \sim \mathcal{N}(\mathbf{0}, \sigma_1^2 I_d)$. We then use *score interpolation* and the learned classifier to gradually denoise the embedding vectors. After the last timestep, we directly infer the generated classes from the predicted feature-specific class probabilities.

3 Continuous Diffusion for Mixed-Type Tabular Data

We combine *score matching* (Eq. (3)) with *score interpolation* (Eq. (4)) to learn the joint distribution of the data from the retrieved score function estimates $\hat{s}_{\text{cont}}^{(i)}$ and $\hat{s}_{\text{cat}}^{(j)}$. An overview of our Continuous Diffusion for Mixed-Type Tabular Data (CDTD) framework is given in Figure 1. The Gaussian noise process acts directly on the continuous features, but on the embeddings of the categorical features. This way, we ensure a common continuous noise process for both data types. The noise processes are directly influenced by (potentially) feature-specific noise levels $\sigma_{\text{cont},i}, \sigma_{\text{cat},j}$ derived from an adaption of timewarping [8] (see following subsections). We adapt the Diffusion Transformer [33] to parameterize the score model and the classifier required for *score interpolation*, and to

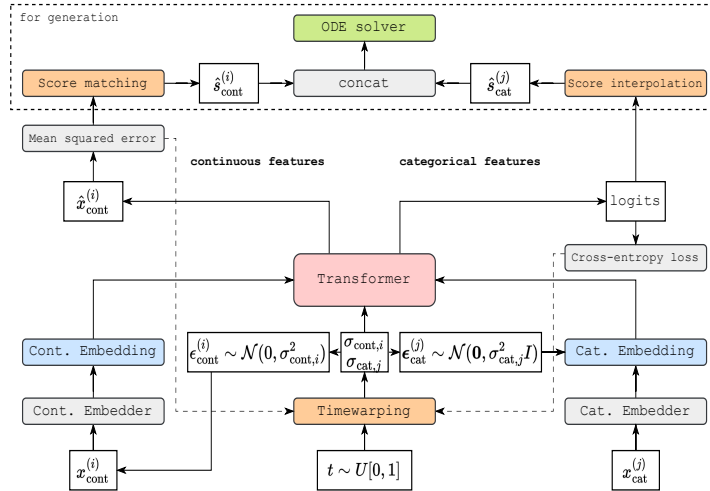


Figure 1: Diffusion for Mixed-Type Tabular Data (CDTD). The left side relates to the score model for continuous features, the right side describes the score interpolation for categorical features. Timewarping allows for a potentially feature-specific, learnable timestep, to diffuse the scalar values (for continuous features) or the embeddings (for categorical features). The approximated score functions are concatenated and passed to a blackbox ODE solver for sample generation.

allow for precise across-type inter-dependencies. The continuous features are embedded in a higher-dimensional space via Fourier features [see also 18, 34]. For categorical features, the typical lookup table is used. The exact implementation details are given in Appendix G.

For continuous features, we use the Transformer output to predict the ground-truth scalar value; for categorical features, the Transformer predicts the class-specific probabilities. The model inputs are the set of noisy scalar values and noisy embeddings for the continuous and categorical features, respectively. We also condition the model on the potentially feature- or type-specific noise at a given timestep. We discuss the exact noise schedule specification in Sections 3.1 and 3.2.

Calibration of Losses. Naturally, the mean squared error (MSE) and the cross-entropy (CE) losses are defined on different scales. During training, the model would therefore treat some features as more important than others, with a potentially negative impact on the overall sample quality. In case of unconditional generation, however, the model should be indifferent between all features a priori, that is, without having any information. This assumption reflects the state of the model at the terminal timestep $t = 1$ for a sufficiently high, unnormalized $t = T$. Hence, we normalize the feature-specific losses by their respective losses under no information: for continuous features, standardization, to have zero mean and unit variance, implies an expected MSE of 1 at $t = 1$; for categorical features, normalization is based on the maximum attainable CE when predicting each class in proportion to its empirical distribution in the train set (for details see, Appendix A). We can then average all losses, regardless of the data type, to derive a joint loss function:

$$\mathcal{L}_{\text{joint}}(\boldsymbol{\theta}) = \frac{1}{K_{\text{cat}} + K_{\text{cont}}} \left[\sum_{i=1}^{K_{\text{cont}}} \ell_{\text{cont}}^{(i)}(\boldsymbol{\theta}) + \sum_{j=1}^{K_{\text{cat}}} \ell_{\text{cat}}^{(j)}(\boldsymbol{\theta}) \right], \quad (5)$$

where $\ell_{\text{cont}}^{(i)}(\boldsymbol{\theta})$ is the *score matching* loss of the i -th continuous feature, and $\ell_{\text{cat}}^{(j)}(\boldsymbol{\theta})$ is the CE loss of the j -th categorical feature. For sampling, the concatenated score function estimates are input to an ODE solver (Euler with 200 steps to minimize the discretization error).

Preprocessing of Continuous Features. In a general tabular data setting, each continuous feature may have a vastly different and likely non-Gaussian distribution. Diffusion models however exhibit an inductive “bias” towards Gaussianity. Therefore, to maximize the generative performance, we transform the continuous distributions to Gaussian-like distributions: for truly continuous features, we use quantile transformation; for continuous features which are inherently discrete and with fully observed possible unique values, we use dequantization. In cases, where most of the probability mass is concentrated in a single value, quantile transformation no longer produces a Gaussian-like distribution. Dequantization helps to learn the distributions of such highly skewed, continuous features. (Note that for a dequantized feature, the model is no longer able to produce predictions outside of the original domain.)

3.1 Feature-specific Noise Schedules

In the case of mixed-type data, for a given embedding dimension, more noise might be needed to remove a given amount of signal from embeddings of features with fewer categories. Thus, it is unlikely that a single noise schedule is optimal for all features. We therefore investigate the following specifications: (1) feature-specific adaptive noise schedules, (2) adaptive noise schedules differentiated per data type, and (3) a single adaptive noise schedule for both types.

For brevity, we only introduce the feature-specific noise schedules explicitly. The other noise schedule types are easily derived from our argument by appropriately combining terms. We let the i -th continuous feature follow the diffusion process:

$$dx_{\text{cont}}^{(i)} = f_{\text{cont},i}(x_{\text{cont}}^{(i)}, t)dt + g_{\text{cont},i}(t)dw_t^{(i)}, \quad (6)$$

and describe the trajectory of the embedding of the j -th categorical feature as

$$d\mathbf{x}_{\text{cat}}^{(j)} = \mathbf{f}_{\text{cat},j}(\mathbf{x}_{\text{cat}}^{(j)}, t)dt + g_{\text{cat},j}(t)d\mathbf{w}_t^{(j)}, \quad (7)$$

where $\mathbf{x}_{\text{cat}}^{(j)}$ represents the d -dimensional embedding of $x_{\text{cat}}^{(j)}$ in Euclidean space.

We follow the EDM specification of Karras et al. [23] and set $f_{\text{cont},i}(x_{\text{cont}}^{(i)}, t)$ and $\mathbf{f}_{\text{cat},j}(\mathbf{x}_{\text{cat}}^{(j)}, t)$ to zero, and the feature-specific diffusion coefficients to $g_{\text{cont},i}(t) = \sqrt{2\sigma_{\text{cont},i}(t)}$ and $g_{\text{cat},j}(t) = \sqrt{2\sigma_{\text{cat},j}(t)}$.

$\sigma_{\text{cont},i}(t)$ and $\sigma_{\text{cat},j}(t)$ are the standard deviations of the Gaussian noise added to the i -th continuous feature and the embedded j -th categorical feature such that $x_{\text{cont},t}^{(i)} \sim \mathcal{N}(x_{\text{cont},0}^{(i)}, \sigma_{\text{cont},i}(t)^2)$ and $\mathbf{x}_{\text{cat},t}^{(j)} \sim \mathcal{N}(\mathbf{x}_{\text{cat},0}^{(j)}, \sigma_{\text{cat},j}(t)^2 I_d)$, respectively. Thus, each continuous feature is governed by a distinct, individual noise schedule (and therefore SDE), whereas all elements of an embedding associated with a given categorical feature follow the same noise schedule.

Since in the forward process, we add noise directly to the continuous features but to the embeddings of categorical features, we generally need much more noise to remove all signal from the categorical representations. In practice, we therefore define the type-specific minimum and maximum noise levels to be $\sigma_{\text{cat},\min} = \sigma_{\text{cat},i}(0) = 0.1$ for all j and $\sigma_{\text{cat},\max} = \sigma_{\text{cat},j}(1) = 200$; and follow [23] and set $\sigma_{\text{cont},\min} = \sigma_{\text{cont},i}(0) = 0.002$ and $\sigma_{\text{cont},\max} = \sigma_{\text{cont},i}(1) = 80$ for all i .

3.2 Adaptive Noise Schedules

The noise schedule determination for mixed-type tabular data is challenging: we have to reconcile two different types of data with a different sensitivity to additive noise. Adaptive noise schedules avoid an explicit formulation of schedules and timestep weights, that is, the model learns to automatically weight those noise levels higher, which are most important for the generative, reverse process [8]. This also makes training (and generation) more efficient: the model spends more time on important noise levels, and the generative capacity gets allocated more optimally.

We start with learning a function $h_k : \sigma_k \mapsto \ell_k$, alongside the diffusion model, to predict the relevant diffusion loss ℓ_k for each feature k . Note that ℓ_k does not include any explicit weighting of the loss over timesteps, and σ_k can be scaled to be in the interval $[0, 1]$. Since a larger noise level implies a lower signal-to-noise ratio, and therefore a larger incurred loss for the score model, f_k must be a monotonically increasing, S-shaped function. Therefore, we let $h_k(\sigma_k) = \gamma_k F_k(\sigma_k)$, where $F_k : [0, 1] \mapsto [0, 1]$ is the domain-adapted Logistic cumulative distribution function, and γ_k is a scaling factor that enables h_k to fit losses different from 1 at the terminal timestep (for the full derivation of h_k see, Appendix B).

Without loss of generality, at each training step, we sample a time $t \sim \mathcal{U}_{[0,1]}$ and determine $\sigma(t) \in \{\sigma_{\text{cont},1}(t), \dots, \sigma_{\text{cont},K_{\text{cont}}}(t), \sigma_{\text{cat},1}(t), \dots, \sigma_{\text{cat},K_{\text{cat}}}(t)\}$. For this, we let $\gamma_k = 1$ such that $h_k^{-1} = F_k^{-1}$ is the quantile function or inverse cdf. Like the original timewarping, this transformation pushes the respective diffusion losses towards evolving linearly in time. Given the limited flexibility of h_k , however, this never occurs in practice and we found this to benefit sample quality. We apply the learned noise schedules both during training and generation. The weighting of each timestep is shown in the pdf of the distribution. We avoid h_k to become biased towards timesteps that are frequently sampled during training by fitting h_k using importance weights derived from the pdf [8].

Our functional choice has several advantages. First, each h_k only requires the estimation of two additional parameters μ_k , the location of the inflection point, and the steepness of the curve ν_k . Second, these parameters are well interpretable in the diffusion context and provide some information on the inner workings of the model. For instance, if $\mu_1 < \mu_2$, the reverse process starts generating feature 2 before feature 1. Note that this functional form is much less flexible than a piece-wise linear function, such that an exponential moving average on the parameters is unnecessary. Lastly, the quantile function as well as the pdf are available in closed form, and therefore no approximations are required.

4 Experiments

We benchmark our model against several popular generative models and across multiple datasets. In addition, we investigate three different (adaptive) noise schedule specifications: (1) feature-specific adaptive noise schedules (*per feature*), (2) adaptive noise schedules differentiated per data type (*per type*), or (3) a single adaptive noise schedule for both types (*single*).

Baseline models. We benchmark our model against several state-of-the-art generative models for mixed-type tabular data, each of which with a different design and / or modeling philosophy. This includes ARF [35], CTGAN [29], TVAE [29], and TabDDPM [24]. Further details are provided in Appendix C.

Datasets. We consider six different datasets to systematically investigate our model. The datasets vary in size, prediction task (regression vs. binary classification), number of features and their distributions. Particularly for categorical features, the number of categories varies significantly across datasets (for more details see, Appendix E). We remove observations with missings in the target or any of the continuous features, and encode missings in the categorical features as a separate category. All datasets are split in 60% train, 20% validation and 20% test partitions. For classification task datasets, we use stratification with respect to the outcome, and we condition the model on the outcome during training and generation which we generate using the train set proportions. For all models, we round the integer-valued continuous features.

Tuning framework. For hyperparameter tuning on a common objective, we follow Kotelnikov et al. [24] and first tune a catboost model for 100 trials on the real data and the data-specific prediction task. The tuned catboost model is then used to tune the generative model for 25 trials. In each trial, we sample a synthetic dataset of the same size as the real dataset and optimize the machine learning efficiency (see Section 4.1) that the tuned catboost model, trained on the generated data, achieves on the real validation set. For more details see Appendix D.

4.1 Evaluation Metrics

We evaluate all generative models on four criteria. We briefly discuss the selected criteria below. All metrics are averaged over five random seeds that affect the generative process. We generate a synthetic dataset of the same size as the real train set to evaluate the machine learning efficiency, statistical similarity and distance to closest record.

Machine learning efficiency. We train a group of models, consisting of a (logistic) regression, a tree, a random forest and a (tuned) catboost model, on the data-specific prediction task. The hyperparameter settings for these machine learning efficiency models are reported in Appendix F. The models’ average real test set performance is compared when trained on the real training set or a synthetic training set [see also, 24, 26, 29, 35–37]. The results are averaged over ten different model seeds (in addition to the five random seeds that impact the sampling process). For brevity, we only report the absolute differences of these performances in the main part of this paper. For regression tasks, we consider the RMSE and the R^2 score; and for classification tasks, the accuracy, macro-averaged F1, and Brier scores.

Detection score. For each generative model, we report the accuracy of a catboost model that is trained to distinguish between real and generated (fake) samples [36, 37]. The train, validations and test sets contain equal proportions of real and fake samples. To constrain the evaluation time, we subsample the real data subsets to not contain more than 25 000 data samples each. We tune each catboost model on the validation set and report the accuracy of the best-fitting model on the test set (see Appendix D for more details). A perfect detection score would be 0.5, indicating that the model is indifferent between fake and real samples.

Statistical similarity. We evaluate the statistical similarity between real and generated training data based on: (1) the Jensen-Shannon divergence (JSD) [38] to quantify the difference in categorical distributions, (2) the Wasserstein distance (WD) [39] to quantify the difference in continuous distributions, and (3) the L_2 norm of the differences of the pair-wise correlation matrices. For the correlations between two continuous features, we use the Pearson correlation coefficient; for the correlations between two categorical features, the Theil uncertainty coefficient and across types the correlation ratio [24, 40] is used.

Distance to closest record (DCR). The DCR of a given generated data point is the minimum Euclidean distance of that data point to all observations in the (possibly subsampled) true training set [36, 40]. We one-hot encode categorical features and standardize all features to zero mean and unit variance, to ensure that each feature contributes equally to the distance. We compute the average DCR as a robust estimate. For brevity, we take the difference of the DCR for the synthetic data and the DCR of the real test set. Hence, a good DCR value should be non-negative and not too high in magnitude.

Table 1: Model evaluation results averaged over six datasets for four benchmark models and for CDTD with three different noise schedules.

	ARF	CTGAN	TVAE	TabDDPM	CDTD (single)	CDTD (per type)	CDTD (per feature)
Accuracy (abs. diff.; ↓)	0.009	0.012	0.009	0.003	0.003	0.002	0.003
F1 (abs. diff.; ↓)	0.019	0.020	0.011	0.003	0.005	0.003	0.004
Brier (abs. diff.; ↓)	0.003	0.006	0.005	0.001	0.001	0.001	0.001
L ₂ distance (↓)	0.731	0.943	1.286	1.803	0.351	0.309	0.316
DCR diff. to test set	0.725	1.133	0.580	0.093	-0.088	0.015	0.089
WD (↓)	0.006	0.071	0.082	0.025	0.012	0.011	0.012
JSD (↓)	0.011	0.015	0.018	0.021	0.004	0.003	0.004
Detection Score (↓)	0.946	0.983	0.969	0.749	0.776	0.748	0.766
RMSE (abs. diff.; ↓)	0.047	0.096	0.109	0.314	0.029	0.052	0.057
R ² (abs. diff.; ↓)	0.035	0.055	0.080	0.066	0.026	0.025	0.024

4.2 Results

Table 1 shows the estimated sample quality measures averaged across all datasets for the four benchmark models and for CDTD with three different noise schedule specifications. For the accuracy, F1 and Brier scores, the results are averaged over the classification task datasets. Likewise, the RMSE and R² averages include the regression task datasets only. The individual, dataset-specific results (including standard errors) are collected in Appendix H. The CDTD training times, despite using a transformer backend, are competitive: Our model samples 1,000 data points in 1.39 sec (averaged over all datasets). This is (over) twice as fast as TabDDPM (3.81 sec) but as expected behind CTGAN (0.14 sec) and TVAE (0.07 sec).

Our CDTD model also consistently outperforms the selected benchmarks in most evaluation metrics, and often even substantially. Specifically, CDTD either outperforms or performs on par with TabDDPM. The latter also requires a (much) high number of parameters to keep up with CDTD. Explicitly accounting for heterogeneity in the noise schedule specification seems to be valuable to a certain extent. We see that type-specific noise schedules outperform both single and feature-specific noise schedules on most metrics. The L₂ norm results of the differences in the correlation matrices of the real and synthetic train sets are outstanding, and demonstrate the benefit to sample quality of pushing the diffusion of categorical features into embedding space. The statistical similarity of the generated categorical features is competitive, even when compared to the ARF benchmark, a tree-based method known to have a (positive) performance bias to categorical data. The DCR results indicate no privacy issues or copying of training samples, as all values are either positive or only marginally negative.

5 Conclusion and Discussion

In summary, we have proposed a continuous diffusion model for mixed-type tabular data that combines score matching and score interpolation. This ensures a common type of noise distribution for both continuous and categorical features and allows the application of diffusion-related advances from the image domain to tabular data. Further, we investigate the use of adaptive, type- or feature-specific noise schedules to account for the high feature heterogeneity in tabular data compared to images. Our results show that the CDTD model outperforms the benchmark models on most metrics, often with a large margin, and that accounting for type-specific heterogeneity in the noise schedules benefits sample quality.

6 Acknowledgements

This work used the Dutch national e-infrastructure with the support of the SURF Cooperative using grant no. EINF-7437.

References

- [1] Yang Song, Jascha Sohl-Dickstein, Diederik P. Kingma, Abhishek Kumar, Stefano Ermon, and Ben Poole. Score-Based Generative Modeling through Stochastic Differential Equations. In *ICLR*, 2021.
- [2] Jascha Sohl-Dickstein, Eric A. Weiss, Niru Maheswaranathan, and Surya Ganguli. Deep Unsupervised Learning using Nonequilibrium Thermodynamics. In *Proceedings of the 32nd International Conference on Machine Learning*, volume 37, Lille, France, 2015. JMLR.
- [3] Jonathan Ho, Ajay Jain, and Pieter Abbeel. Denoising Diffusion Probabilistic Models. In *Advances in Neural Information Processing Systems*, volume 33, pages 6840–6851. Curran Associates, Inc., 2020.
- [4] Prafulla Dhariwal and Alex Nichol. Diffusion Models Beat GANs on Image Synthesis. In *Advances in Neural Information Processing Systems*, volume 34, pages 8780–8794. Curran Associates, Inc., 2021.
- [5] Robin Rombach, Andreas Blattmann, Dominik Lorenz, Patrick Esser, and Björn Ommer. High-Resolution Image Synthesis with Latent Diffusion Models. *arXiv preprint arXiv:2112.10752*, 2022.
- [6] Jonathan Ho, Tim Salimans, Alexey Gritsenko, William Chan, Mohammad Norouzi, and David J. Fleet. Video Diffusion Models. *arXiv preprint arXiv:2204.03458*, 2022.
- [7] Xiang Lisa Li, John Thickstun, Ishaan Gulrajani, Percy Liang, and Tatsunori B. Hashimoto. Diffusion-LM Improves Controllable Text Generation. *arXiv preprint arXiv:2205.14217*, 2022.
- [8] Sander Dieleman, Laurent Sartran, Arman Roshannai, Nikolay Savinov, Yaroslav Ganin, Pierre H. Richemond, Arnaud Doucet, Robin Strudel, Chris Dyer, Conor Durkan, Curtis Hawthorne, Rémi Leblond, Will Grathwohl, and Jonas Adler. Continuous diffusion for categorical data. *arXiv preprint arXiv:2211.15089*, 2022.
- [9] Tong Wu, Zhihao Fan, Xiao Liu, Yeyun Gong, Yelong Shen, Jian Jiao, Hai-Tao Zheng, Juntao Li, Zhongyu Wei, Jian Guo, Nan Duan, and Weizhu Chen. AR-Diffusion: Auto-Regressive Diffusion Model for Text Generation. *arXiv preprint arXiv:2305.09515*, 2023.
- [10] Emiel Hoogeboom, Victor Garcia Satorras, Clément Vignac, and Max Welling. Equivariant Diffusion for Molecule Generation in 3D. In *Proceedings of the 39th International Conference on Machine Learning*, volume 162 of *Proceedings of Machine Learning Research*, pages 8867–8887, Baltimore, Maryland, USA, 2022. PMLR.
- [11] Jacob Austin, Daniel D. Johnson, Jonathan Ho, Daniel Tarlow, and Rianne van den Berg. Structured Denoising Diffusion Models in Discrete State-Spaces. *arXiv preprint arXiv:2107.03006*, 2021.
- [12] Emiel Hoogeboom, Didrik Nielsen, Priyank Jaini, Patrick Forré, and Max Welling. Argmax Flows and Multinomial Diffusion: Learning Categorical Distributions. In *Advances in Neural Information Processing Systems*, volume 34, pages 12454–12465. Curran Associates, Inc., 2021.
- [13] Florence Regol and Mark Coates. Diffusing Gaussian Mixtures for Generating Categorical Data. *Proceedings of the AAAI Conference on Artificial Intelligence*, 37(8):9570–9578, 2023. ISSN 2374-3468, 2159-5399. doi: 10.1609/aaai.v37i8.26145.
- [14] Robin Strudel, Corentin Tallec, Florent Alché, Yilun Du, Yaroslav Ganin, Arthur Mensch, Will Grathwohl, Nikolay Savinov, Sander Dieleman, Laurent Sifre, and Rémi Leblond. Self-conditioned Embedding Diffusion for Text Generation. *arXiv preprint arXiv:2211.04236*, 2022.
- [15] Andrew Campbell, Joe Benton, Valentin De Bortoli, Tom Rainforth, George Deligiannidis, and Arnaud Doucet. A Continuous Time Framework for Discrete Denoising Models. In *Advances in Neural Information Processing Systems*, volume 35, New Orleans, USA, 2022.
- [16] Chenlin Meng, Kristy Choi, Jiaming Song, and Stefano Ermon. Concrete Score Matching: Generalized Score Matching for Discrete Data. In *Advances in Neural Information Processing Systems*, volume 35, pages 34532–34545. Curran Associates, Inc., 2022.
- [17] Haoran Sun, Lijun Yu, Bo Dai, Dale Schuurmans, and Hanjun Dai. Score-based Continuous-time Discrete Diffusion Models. *arXiv preprint arXiv:2211.16750*, 2023.
- [18] Diederik P. Kingma, Tim Salimans, Ben Poole, and Jonathan Ho. Variational Diffusion Models. *arXiv preprint arXiv:2107.00630*, 2022.
- [19] Ting Chen, Ruixiang Zhang, and Geoffrey Hinton. Analog Bits: Generating Discrete Data using Diffusion Models with Self-Conditioning. *arXiv preprint arXiv:2208.04202*, 2022.

- [20] Ting Chen. On the Importance of Noise Scheduling for Diffusion Models. *arXiv preprint arXiv:2301.10972*, 2023.
- [21] Allan Jabri, David Fleet, and Ting Chen. Scalable Adaptive Computation for Iterative Generation. *arXiv preprint arXiv:2212.11972*, 2022.
- [22] Alex Nichol and Prafulla Dhariwal. Improved Denoising Diffusion Probabilistic Models. In *Proceedings of the 38th International Conference on Machine Learning*, volume 139. PMLR, 2021.
- [23] Tero Karras, Miika Aittala, Timo Aila, and Samuli Laine. Elucidating the Design Space of Diffusion-Based Generative Models. In *Advances in Neural Information Processing Systems*, volume 35, pages 26565–26577. Curran Associates, Inc., 2022.
- [24] Akim Kotelnikov, Dmitry Baranchuk, Ivan Rubachev, and Artem Babenko. TabDDPM: Modelling Tabular Data with Diffusion Models. In *Proceedings of the 40th International Conference on Machine Learning*, volume 202 of *Proceedings of Machine Learning Research*, pages 17564–17579. PMLR, 2023.
- [25] Chaejeong Lee, Jayoung Kim, and Noseong Park. CoDi: Co-evolving Contrastive Diffusion Models for Mixed-type Tabular Synthesis. In *Proceedings of the 40th International Conference on Machine Learning*, volume 202, Honolulu, Hawaii, USA, 2023. PMLR.
- [26] Jayoung Kim, Chaejeong Lee, and Noseong Park. STaSy: Score-based Tabular data Synthesis. *arXiv preprint arXiv:2210.04018*, 2023.
- [27] Cheng Lu, Yuhao Zhou, Fan Bao, Jianfei Chen, Chongxuan Li, and Jun Zhu. DPM-Solver: A Fast ODE Solver for Diffusion Probabilistic Model Sampling in Around 10 Steps. In *36th Conference on Neural Information Processing Systems*, 2022.
- [28] Jonathan Ho and Tim Salimans. Classifier-Free Diffusion Guidance. *arXiv preprint arXiv:2207.12598*, 2022.
- [29] Lei Xu, Maria Skoularidou, Alfredo Cuesta-Infante, and Kalyan Veeramachaneni. Modeling Tabular Data using Conditional GAN. In *Advances in Neural Information Processing Systems*, volume 12. Curran Associates, Inc., 2019.
- [30] Aapo Hyvärinen. Estimation of Non-Normalized Statistical Models by Score Matching. *Journal of Machine Learning Research*, 6(24):695–709, 2005.
- [31] Georgios Batzolis, Jan Stanczuk, Carola-Bibiane Schönlieb, and Christian Etmann. Non-Uniform Diffusion Models. *arXiv preprint arXiv:2207.09786*, 2022.
- [32] Pascal Vincent. A Connection Between Score Matching and Denoising Autoencoders. *Neural Computation*, 23(7):1661–1674, 2011. ISSN 0899-7667, 1530-888X. doi: 10.1162/NECO_a_00142.
- [33] William Peebles and Saining Xie. Scalable Diffusion Models with Transformers. *arXiv preprint arXiv:2212.09748*, 2023.
- [34] Yury Gorishniy, Ivan Rubachev, and Artem Babenko. On Embeddings for Numerical Features in Tabular Deep Learning. *arXiv preprint arXiv:2203.05556*, 2022.
- [35] David S. Watson, Kristin Blesch, Jan Kapar, and Marvin N. Wright. Adversarial random forests for density estimation and generative modeling. In *Proceedings of the 26th International Conference on Artificial Intelligence and Statistics*, volume 206, Valencia, Spain, 2023. PMLR.
- [36] Vadim Borisov, Kathrin Seßler, Tobias Leemann, Martin Pawelczyk, and Gjergji Kasneci. Language Models are Realistic Tabular Data Generators. In *International Conference on Learning Representations*, 2023.
- [37] Tennison Liu, Zhaozhi Qian, Jeroen Berrevoets, and Mihaela van der Schaar. GOGGLE: Generative Modelling for Tabular Data by Learning Relational Structure. In *International Conference on Learning Representations*, 2023.
- [38] Jianhua Lin. Divergence Measures Based on the Shannon Entropy. *IEEE Transactions on Information Theory*, 37(1):145–151, 1991.
- [39] Aaditya Ramdas, Nicolas Garcia, and Marco Cuturi. On Wasserstein Two Sample Testing and Related Families of Nonparametric Tests. *Entropy*, 19(2), 2017.

- [40] Zilong Zhao, Aditya Kumar, Hiek Van der Scheer, Robert Birke, and Lydia Y. Chen. CTAB-GAN: Effective Table Data Synthesizing. In *Proceedings of the 13th Asian Conference on Machine Learning*, volume 157, pages 97–112. PMLR, 2021.
- [41] Liudmila Prokhorenkova, Gleb Gusev, Aleksandr Vorobev, Anna Veronika Dorogush, and Andrey Gulin. CatBoost: Unbiased boosting with categorical features. In *Advances in Neural Information Processing Systems*, volume 31. Curran Associates, Inc., 2018.
- [42] Takuya Akiba, Shotaro Sano, Toshihiko Yanase, Takeru Ohta, and Masanori Koyama. Optuna: A next-generation hyperparameter optimization framework. In *Proceedings of the 25th ACM SIGKDD International Conference on Knowledge Discovery & Data Mining*, KDD '19, page 2623–2631, New York, NY, USA, 2019. Association for Computing Machinery.
- [43] Barry Becker and Ronny Kohavi. Adult. UCI Machine Learning Repository, 1996. DOI: <https://doi.org/10.24432/C5XW20>.
- [44] S. Moro, P. Rita, and P. Cortez. Bank Marketing. UCI Machine Learning Repository, 2012. DOI: <https://doi.org/10.24432/C5K306>.
- [45] Song Chen. Beijing PM2.5 Data. UCI Machine Learning Repository, 2017. DOI: <https://doi.org/10.24432/C5JS49>.
- [46] Iranian Churn Dataset. UCI Machine Learning Repository, 2020. DOI: <https://doi.org/10.24432/C5JW3Z>.
- [47] I-Cheng Yeh. Default of credit card clients. UCI Machine Learning Repository, 2016. DOI: <https://doi.org/10.24432/C55S3H>.
- [48] Partha Deb and Pravin K. Trivedi. Demand for Medical Care by the Elderly: A Finite Mixture Approach. *Journal of Applied Econometrics*, 12(3):313–336, 1997. ISSN 0883-7252, 1099-1255. doi: 10.1002/(SICI)1099-1255(199705)12:3<313::AID-JAE440>3.0.CO;2-G.

A Calibration of Losses

If a continuous and a categorical feature incur the same loss and both losses are improved by 1%, we want to ensure that this reflects the same improvement in “goodness of fit” for both features. To achieve a calibration between the losses of the two different data types, we let the model be indifferent between features a priori, i.e., the features should attain the same loss at the terminal timestep $t = T$. With T sufficiently large, the signal-to-noise ratio is sufficiently low to approximate a situation in which the model has no information about the data.

In case of a continuous feature and no prior information, it is optimal for the model to always predict the average value $\mathbb{E}[x_{\text{cont}}^{(i)}]$ for all $x_{\text{cont},j}^{(i)}$, where j indexes the individual observations in the i.i.d. sample. Then, the MSE loss becomes:

$$\begin{aligned} \mathbb{E}\left[\frac{1}{N}\sum_j(x_{\text{cont},j}^{(i)} - \hat{x}_{\text{cont},j}^{(i)})^2\right] &= \mathbb{E}\left[\frac{1}{N}\sum_j(x_{\text{cont},j}^{(i)} - \mathbb{E}[x_{\text{cont}}^{(i)}])^2\right] \\ &= \mathbb{E}[(x_{\text{cont},j}^{(i)} - \mathbb{E}[x_{\text{cont}}^{(i)}])^2] \\ &= \text{Var}[x_{\text{cont},j}^{(i)}] \\ &= \text{Var}[x_{\text{cont}}^{(i)}] = 1. \end{aligned}$$

The last line assumes standardized data (i.e., to have zero mean and unit variance). This results (approximately) in a loss of one for all continuous features at $t = T$.

For a categorical feature, $x_{\text{cat},j}^{(i)}$ distributed according to empirical proportions p_k for $k = 1, \dots, K$ categories, we are interested in the cross-entropy loss of our predicted class probabilities q_k . With no information, it is optimal for the model to predict the k -th category in the same proportion as it appears in the training set. Thus, we let $q_k = p_k$ and obtain

$$\mathbb{E}\left[-\sum_k I(x_{\text{cat},j}^{(i)} = k) \log q_k\right] = \mathbb{E}\left[-\sum_k p_k \log p_k\right].$$

To achieve a cross-entropy loss of one at the terminal timestep, we divide the feature-specific cross-entropy losses by the sample estimate of the maximum attainable cross-entropy under no information given above. Given these adjustments, for parameters in a (or close to a) local optimum, we therefore have that $0 \leq \ell_{\text{cont}}^{(m)}(\theta), \ell_{\text{cat}}^{(n)}(\theta) \leq 1$. Note that once we train a conditional score model, some features naturally turn out to be more important or easier to generate than others, due to the interdependence with the conditioning information.

B Derivation of the Timewarping Functional Form

We want to incorporate the prior information about the S-shaped loss in the functional form, while being able to easily invert and differentiate the function. A convenient choice is therefore the cdf, F , of the logistic distribution, for which the derivative is the pdf, f , and the inverse function the inverse cdf or quantile function, F^{-1} . All are attainable without approximations and in closed form, however the domain of F (and co-domain of F^{-1}) is $(-\infty, \infty)$. The cdf of the logistic distribution is

$$F(y) = [1 + \exp(-\nu(y - \mu_0))]^{-1}, \quad (8)$$

where μ^* describes the location of the inflection point of the S-shaped function and $\nu \geq 1$ indicates the steepness of the approximated step function. To change the domain of $F(y)$ to the interval $(0, 1)$, we let $y = \text{logit}(x) = \ln \frac{x}{1-x}$. To define the parameter μ in the same space and ensure that $0 < \mu < 1$, we let $\mu^* = \text{logit}(\mu)$. With these substitutions and some algebra, we get

$$F(x) = \left[1 + \left(\frac{x}{1-x} \frac{1-\mu}{\mu}\right)^{-\nu}\right]^{-1}. \quad (9)$$

In practice, x represents the noise level, σ , that F takes in to predict the (feature-specific) loss ℓ . Since ℓ is not bounded above, we introduce a multiplicative scale parameter, γ , such that $\hat{\ell} = h(\sigma) = \gamma F(\sigma)$.

We initialize $\mu = 0.5$, $\nu \approx 1$ and $\gamma = 1$, such that F starts (approximately) as the cdf of a uniform distribution, and we therefore sample initially uniformly across all timesteps.

The inverse cdf, $F(t)^{-1}$, can also be derived in closed form and is given by $x = \text{sigmoid}(c)$, with

$$c = \ln\left(\frac{\mu}{1-\mu}\right) + \frac{1}{\nu} \ln\left(\frac{t}{1-t}\right). \quad (10)$$

We learn the parameters, μ, ν and γ , by predicting the (feature-specific) loss using $h(\sigma)$ with the noise levels scaled to $(0, 1)$ as the input. At the beginning of each training step of the score model, we then use the current state of these parameters and the inverse function, F^{-1} , with timestep $t \sim \mathcal{U}_{[0,1]}$ as the input, to derive the optimal noise level, σ . Since we create a feedback loop when using timewarping to generate more σ s from the regions of interest, we follow Dieleman et al. [8] and weight the timewarping loss, $\|\ell - \hat{\ell}\|_2^2$, by the reciprocal of the pdf, $f(x)$. Again, this function is available to us in closed form.

Let F_{logistic} and f_{logistic} denote the cdf and pdf of the Logistic distribution, respectively. With $y = \ln \frac{x}{1-x}$, we can derive the pdf of interest as

$$\begin{aligned} f(x) &= \frac{\partial}{\partial y} F_{\text{logistic}}(y) \frac{\partial}{\partial x} \ln \frac{x}{1-x} \\ &= f_{\text{logistic}}(y) \frac{1}{x(1-x)}. \end{aligned}$$

We can then plug in the known form of $f_{\text{logistic}}(y)$ and use our definitions of y and the parameters μ and ν to get

$$f(x) = \frac{\nu}{x(1-x)} \cdot \frac{Z(x, \mu, \nu)}{1 + Z(x, \mu, \nu)^2}, \quad (11)$$

with $Z(x, \mu, \nu) = \left(\frac{x}{1-x} \frac{1-\mu}{\mu}\right)^{-\nu}$.

C Baseline Models

We compare our model to a number of generative models specifically designed for modeling mixed-type tabular data:

- ARF [35] – a very recent generative approach that is based on a random forest for density estimation.
- CTGAN [29] – one of the most popular Generative-Adversarial-Network-based models for tabular data (the implementation is available at <https://github.com/sdv-dev/CTGAN>).
- TVAE [29] – a Variational-Autoencoder-based model for tabular data (the implementation is available at <https://github.com/sdv-dev/CTGAN>).
- TabDDPM [24] – a diffusion-based generative model for tabular data that combines multinomial diffusion [12] and diffusion in continuous space.

Table 2: Hyperparameter space settings for CDTD (ours). The model is tuned for 25 trials.

Parameter	Distribution
embedding dimension	Cat([64, 128])
cat embedding σ_{init}	Cat([0.001, 0.01, 0.1])
batch size	= min(4096, train set size)
no. train steps	Cat([10000, 15000, 20000])
learning rate	Log Uniform [0.0001, 0.002]
depth	Cat([2, 3, 4])
heads	Cat([4, 8, 16])
weight decay	Cat([0, 1e-3])

Table 3: Settings of the hyperparameter space for ARF [35]. The model is tuned for 25 trials.

Parameter	Distribution
minimum node size	Cat([5,10,15,20])
maximum iters	Cat([10, 20, 30, 50])
no. trees	Cat([30, 50, 70, 90])

Table 4: Settings of the hyperparameter space for CTGAN [29]. The model is tuned for 25 trials.

Parameter	Distribution
embedding dimension	Cat([128, 256, 512])
batch size	= min(4096, train set size)
no. train steps	Cat([10000, 15000, 20000])
no. layers	Cat([1,2,3,4,5])
generator/discriminator dimension	Cat([128, 256, 512])
learning rate generator/discriminator	Log Uniform [1e-4, 2e-3]

Table 5: Settings of the hyperparameter space for TVAE [29]. The model is tuned for 25 trials.

Parameter	Distribution
embedding dimension	Cat([128, 256, 512])
batch size	= min(4096, train set size)
no. train steps	Cat([10000, 15000, 20000])
loss factor	Log Uniform [1, 5]
no. layers	Cat([1,2,3,4,5])
encoder/decoder dimension	Cat([128, 256, 512])
learning rate	Log Uniform [1e-4, 2e-3]

Table 6: Settings of the hyperparameter space for TabDDPM [24]. The model is tuned for 25 trials.

Parameter	Distribution
no. train steps	Cat([10000, 15000, 20000])
no. timesteps	= 1000
batch size	= min(4096, train set size)
learning rate	Log Uniform [0.0001, 0.003]
no. hidden layers	Cat([1,2,3,4])
hidden size	Cat([256, 512, 1024])

Table 7: Settings of the hyperparameter space for Catboost [41]. For the machine learning efficiency estimation, we tune the model for 100 trials. When used as a detection model, we tune it for 25 trials.

Parameter	Distribution
no. iterations	= 1000
learning rate	Log Uniform [0.001, 1.0]
depth	Cat([3,4,5,6,7,8])
L2 regularization	Uniform [0.1, 10]
bagging temperature	Uniform [0, 1]
leaf estimation iters	Integer Uniform [1, 10]

D Tuning Setup

D.1 Tuning of the Generative Models

We tune the hyperparameters of all generative models on the fit of the generated samples to the joint distribution of the real training data [24]. This way we ensure all models are tuned on a common objective.

For a given dataset, we first tune a catboost model [41] that predicts the dataset-specific (continuous or binary) target based on the real training set. For regression tasks, we determine the fit based on the RMSE; for binary or multi-class classification, we use the macro-averaged F1-score. We use 5 fold cross-validation on the real training set for estimation; and optuna [42] and 100 trials for tuning.

The best-fitting catboost model for a dataset is used for hyperparameter tuning of each generative model. After model training, we generate a sample of the same size as the real training set for a given set of hyperparameters. We check the models’ machine learning efficiency with the tuned catboost model, i.e., we use the generated data as a drop-in replacement for the real train set and train the catboost model (with the tuned dataset-specific hyperparameters) to predict the outcome in a separate, real data validation set. The tuning objective is derived by averaging the machine learning efficiency over five different seeds that affect the sampling process of the generative models. Again, we use optuna and train each model for 25 trials.

D.2 Tuning of the Detection Model

We again use a catboost model (and optuna with 25 trials for tuning) to test whether real and generated samples can be distinguished. We generate the same number of fake observations for each of the real train, validation and test sets. (We cap the maximum size of the real data subsets to 25,000, and subsample them if necessary, to reduce computation time.) We then combine real and fake observations per set to $\mathcal{D}_{\text{train,detect}}$, $\mathcal{D}_{\text{val,detect}}$ and $\mathcal{D}_{\text{test,detect}}$, respectively. The catboost model is trained on $\mathcal{D}_{\text{train,detect}}$ with the task of predicting whether an observation is real or fake. We evaluate the performance and tune the catboost model in terms of accuracy on $\mathcal{D}_{\text{val,detect}}$. After tuning, the performance of the tuned model on the held-out test set, $\mathcal{D}_{\text{test,detect}}$ gives the estimated detection score.

E Datasets

Table 8: Overview of the experimental datasets. We count the outcome towards the respective features that remain after removing continuous features with an excessive number of missings.

Dataset	Prediction task	Total no. observations	No. categorical features	No. continuous features
adult [43]	binary classification	48 842	9	6
bank [44]	binary classification	41 188	11	10
beijing [45]	regression	41 757	1	10
churn [46]	binary classification.	3 150	5	9
default [47]	binary classification	30 000	10	14
nmes [48]	regression	4 406	8	11

F Machine Learning Efficiency Models

For the group of machine learning efficiency models, we use the scikit-learn and catboost package implementations including the default parameter settings (if not otherwise specified):

- Tree: max_depth = 10
- Random Forest: max_depth = 12, n_estimators = 100
- Logistic or Ridge Regression: max_iter = 1000
- Catboost: tuned on the hyperparameter space reported in Table 7

G Implementation Details

In the Transformer, we embed the timesteps and add them to the respective feature embeddings. Following Dieleman et al. [8], it is crucial to L_2 normalize the embeddings each time we use them, to prevent a degenerate embedding space, in which embeddings are pushed further and further apart. In a conditional model, where we condition the score model on the target feature in the dataset, we use adaptive layer norms [33]. We also use self-conditioning [19] for both types of features. For continuous features we simply condition on the predictions from the previous step, for categorical features we condition on the interpolated embedding. We use an exponential moving average on the parameters of the score model. To decrease the variance of the loss, we use the low-discrepancy sampler to sample $t \sim \mathcal{U}_{[0,1]}$ [18]. For the EDM-specific hyperparameter, σ_{data} , we differentiate between the two data types. Hence, we let $\sigma_{\text{cat,data}} = 1$ and derive $\sigma_{\text{cont,data}}$ from the standard deviation of the preprocessed training data, which should be approximately 1.

H Detailed Results

Table 9: L_2 norm (incl. standard errors in subscripts) of the correlation matrix differences of real and synthetic train sets for four benchmark models and for CDTD with three different noise schedules.

	ARF	CTGAN	TVAE	TabDDPM	CDTD (single)	CDTD (per type)	CDTD (per feature)
adult	0.587 \pm 0.009	0.525 \pm 0.010	0.541 \pm 0.015	0.231 \pm 0.059	0.109 \pm 0.009	0.094 \pm 0.010	0.112 \pm 0.012
bank	0.900 \pm 0.018	0.615 \pm 0.010	1.185 \pm 0.017	1.541 \pm 0.049	0.413 \pm 0.029	0.200 \pm 0.014	0.273 \pm 0.020
churn	0.611 \pm 0.023	0.704 \pm 0.025	1.598 \pm 0.067	0.309 \pm 0.072	0.331 \pm 0.035	0.278 \pm 0.019	0.273 \pm 0.040
default	1.395 \pm 0.022	2.130 \pm 0.035	1.694 \pm 0.033	2.574 \pm 0.091	0.735 \pm 0.046	0.732 \pm 0.046	0.687 \pm 0.051
beijing	0.136 \pm 0.008	1.062 \pm 0.004	1.296 \pm 0.009	1.950 \pm 0.048	0.073 \pm 0.009	0.072 \pm 0.013	0.068 \pm 0.003
nmes	0.759 \pm 0.029	0.624 \pm 0.052	1.401 \pm 0.044	4.209 \pm 0.065	0.442 \pm 0.020	0.480 \pm 0.023	0.484 \pm 0.033

Table 10: Jensen-Shannon divergence (incl. standard errors in subscripts) for four benchmark models and for CDTD with three different noise schedules.

	ARF	CTGAN	TVAE	TabDDPM	CDTD (single)	CDTD (per type)	CDTD (per feature)
adult	0.007 \pm 0.001	0.100 \pm 0.001	0.094 \pm 0.001	0.019 \pm 0.000	0.011 \pm 0.001	0.013 \pm 0.001	0.011 \pm 0.001
bank	0.004 \pm 0.001	0.054 \pm 0.001	0.090 \pm 0.000	0.016 \pm 0.001	0.011 \pm 0.001	0.011 \pm 0.001	0.010 \pm 0.001
churn	0.008 \pm 0.002	0.078 \pm 0.002	0.053 \pm 0.005	0.012 \pm 0.004	0.017 \pm 0.003	0.014 \pm 0.006	0.014 \pm 0.003
default	0.008 \pm 0.001	0.147 \pm 0.001	0.103 \pm 0.001	0.020 \pm 0.001	0.013 \pm 0.001	0.015 \pm 0.002	0.015 \pm 0.002
beijing	0.004 \pm 0.003	0.005 \pm 0.002	0.093 \pm 0.004	0.049 \pm 0.003	0.003 \pm 0.002	0.004 \pm 0.001	0.008 \pm 0.001
nmes	0.006 \pm 0.002	0.040 \pm 0.006	0.060 \pm 0.002	0.033 \pm 0.001	0.017 \pm 0.001	0.009 \pm 0.003	0.013 \pm 0.003

Table 11: Wasserstein distance (incl. standard errors in subscripts) for four benchmark models and for CDTD with three different noise schedules.

	ARF	CTGAN	TVAE	TabDDPM	CDTD (single)	CDTD (per type)	CDTD (per feature)
adult	0.011 \pm 0.000	0.013 \pm 0.000	0.017 \pm 0.000	0.003 \pm 0.000	0.002 \pm 0.000	0.001 \pm 0.000	0.002 \pm 0.000
bank	0.012 \pm 0.000	0.022 \pm 0.000	0.012 \pm 0.000	0.007 \pm 0.001	0.009 \pm 0.001	0.003 \pm 0.000	0.005 \pm 0.000
churn	0.013 \pm 0.001	0.022 \pm 0.001	0.030 \pm 0.001	0.008 \pm 0.001	0.007 \pm 0.001	0.006 \pm 0.000	0.007 \pm 0.001
default	0.005 \pm 0.000	0.014 \pm 0.000	0.014 \pm 0.000	0.007 \pm 0.000	0.002 \pm 0.000	0.002 \pm 0.000	0.002 \pm 0.000
beijing	0.010 \pm 0.000	0.014 \pm 0.000	0.022 \pm 0.000	0.022 \pm 0.000	0.002 \pm 0.000	0.002 \pm 0.000	0.002 \pm 0.000
nmes	0.013 \pm 0.001	0.007 \pm 0.000	0.014 \pm 0.001	0.081 \pm 0.001	0.004 \pm 0.001	0.004 \pm 0.001	0.005 \pm 0.001

Table 12: Detection score (incl. standard errors in subscripts) for four benchmark models and for CDTD with three different noise schedules.

	ARF	CTGAN	TVAE	TabDDPM	CDTD (single)	CDTD (per type)	CDTD (per feature)
adult	0.918 \pm 0.003	0.991 \pm 0.001	0.922 \pm 0.001	0.583 \pm 0.004	0.609 \pm 0.004	0.588 \pm 0.002	0.608 \pm 0.004
bank	0.948 \pm 0.001	1.000 \pm 0.000	1.000 \pm 0.000	0.784 \pm 0.001	0.838 \pm 0.002	0.761 \pm 0.004	0.834 \pm 0.002
churn	0.840 \pm 0.005	0.925 \pm 0.003	0.904 \pm 0.013	0.605 \pm 0.017	0.722 \pm 0.015	0.653 \pm 0.015	0.659 \pm 0.011
default	0.990 \pm 0.001	0.997 \pm 0.001	0.998 \pm 0.000	0.842 \pm 0.002	0.891 \pm 0.001	0.904 \pm 0.002	0.901 \pm 0.003
beijing	0.994 \pm 0.001	0.998 \pm 0.000	0.998 \pm 0.000	0.970 \pm 0.001	0.959 \pm 0.003	0.957 \pm 0.001	0.952 \pm 0.002
nmes	0.987 \pm 0.002	0.988 \pm 0.001	0.991 \pm 0.001	0.714 \pm 0.008	0.635 \pm 0.006	0.626 \pm 0.007	0.642 \pm 0.012

Table 13: Distance to closest record of the generated data (incl. standard errors in subscripts) for four benchmark models and for CDTD with three different noise schedules.

	ARF	CTGAN	TVAE	TabDDPM	CDTD (single)	CDTD (per type)	CDTD (per feature)
adult	2.512 \pm 0.012	3.723 \pm 0.017	2.586 \pm 0.018	1.822 \pm 0.007	2.019 \pm 0.014	1.919 \pm 0.018	2.001 \pm 0.016
bank	3.048 \pm 0.014	3.149 \pm 0.014	3.116 \pm 0.002	2.368 \pm 0.013	2.135 \pm 0.006	2.275 \pm 0.013	2.563 \pm 0.010
churn	1.115 \pm 0.015	1.688 \pm 0.019	1.435 \pm 0.032	0.431 \pm 0.025	0.558 \pm 0.015	0.509 \pm 0.023	0.519 \pm 0.018
default	3.409 \pm 0.025	4.040 \pm 0.022	2.487 \pm 0.024	1.719 \pm 0.019	1.781 \pm 0.022	1.786 \pm 0.018	1.807 \pm 0.018
beijing	0.760 \pm 0.002	0.704 \pm 0.002	0.736 \pm 0.002	0.844 \pm 0.009	0.549 \pm 0.002	0.560 \pm 0.002	0.548 \pm 0.001
nmes	2.224 \pm 0.012	2.210 \pm 0.032	1.835 \pm 0.017	2.089 \pm 0.011	1.145 \pm 0.022	1.755 \pm 0.014	1.813 \pm 0.029

Table 14: Machine learning efficiency accuracy for four benchmark models and for CDTD with three different noise schedules. Standard deviation is computed across the average results of the four machine learning efficiency models.

	ARF	CTGAN	TVAE	TabDDPM	CDTD (single)	CDTD (per type)	CDTD (per feature)
adult	0.848 \pm 0.007	0.842 \pm 0.009	0.847 \pm 0.010	0.854 \pm 0.005	0.855 \pm 0.006	0.856 \pm 0.005	0.854 \pm 0.005
bank	0.907 \pm 0.003	0.908 \pm 0.004	0.908 \pm 0.003	0.912 \pm 0.003	0.910 \pm 0.008	0.913 \pm 0.004	0.913 \pm 0.004
churn	0.907 \pm 0.016	0.888 \pm 0.012	0.904 \pm 0.012	0.937 \pm 0.024	0.936 \pm 0.023	0.936 \pm 0.022	0.931 \pm 0.021
default	0.801 \pm 0.005	0.804 \pm 0.005	0.808 \pm 0.005	0.814 \pm 0.005	0.813 \pm 0.006	0.813 \pm 0.005	0.813 \pm 0.006

Table 15: Machine learning efficiency F1 score for four benchmark models and for CDTD with three different noise schedules. Standard deviation is computed across the average results of the four machine learning efficiency models.

	ARF	CTGAN	TVAE	TabDDPM	CDTD (single)	CDTD (per type)	CDTD (per feature)
adult	0.765 \pm 0.011	0.761 \pm 0.016	0.775 \pm 0.014	0.782 \pm 0.009	0.780 \pm 0.011	0.782 \pm 0.010	0.780 \pm 0.010
bank	0.684 \pm 0.022	0.697 \pm 0.019	0.751 \pm 0.011	0.734 \pm 0.017	0.770 \pm 0.016	0.751 \pm 0.028	0.743 \pm 0.027
churn	0.796 \pm 0.046	0.761 \pm 0.018	0.796 \pm 0.028	0.865 \pm 0.063	0.859 \pm 0.066	0.863 \pm 0.065	0.852 \pm 0.061
default	0.619 \pm 0.016	0.635 \pm 0.012	0.665 \pm 0.010	0.674 \pm 0.007	0.667 \pm 0.008	0.670 \pm 0.007	0.668 \pm 0.007

Table 16: Machine learning efficiency Brier score for four benchmark models and for CDTD with three different noise schedules. Standard deviation is computed across the average results of the four machine learning efficiency models.

	ARF	CTGAN	TVAE	TabDDPM	CDTD (single)	CDTD (per type)	CDTD (per feature)
adult	0.107 \pm 0.004	0.113 \pm 0.009	0.109 \pm 0.009	0.104 \pm 0.005	0.103 \pm 0.005	0.102 \pm 0.004	0.104 \pm 0.005
bank	0.064 \pm 0.004	0.074 \pm 0.011	0.071 \pm 0.009	0.065 \pm 0.005	0.065 \pm 0.011	0.061 \pm 0.006	0.065 \pm 0.006
churn	0.071 \pm 0.016	0.089 \pm 0.018	0.075 \pm 0.018	0.048 \pm 0.015	0.050 \pm 0.015	0.049 \pm 0.014	0.053 \pm 0.015
default	0.148 \pm 0.009	0.163 \pm 0.018	0.164 \pm 0.014	0.143 \pm 0.009	0.143 \pm 0.010	0.143 \pm 0.009	0.143 \pm 0.009

Table 17: Machine learning efficiency RMSE for four benchmark models and for CDTD with three different noise schedules. Standard deviation is computed across the average results of the four machine learning efficiency models.

	ARF	CTGAN	TVAE	TabDDPM	CDTD (single)	CDTD (per type)	CDTD (per feature)
beijing	0.793 \pm 0.061	0.977 \pm 0.039	1.067 \pm 0.064	0.417 \pm 0.044	0.786 \pm 0.072	0.785 \pm 0.072	0.782 \pm 0.074
nmes	0.983 \pm 0.062	0.994 \pm 0.118	1.074 \pm 0.124	0.253 \pm 0.025	1.044 \pm 0.125	1.167 \pm 0.133	1.188 \pm 0.134

Table 18: Machine learning efficiency R² for four benchmark models and for CDTD with three different noise schedules. Standard deviation is computed across the average results of the four machine learning efficiency models.

	ARF	CTGAN	TVAE	TabDDPM	CDTD (single)	CDTD (per type)	CDTD (per feature)
beijing	0.387 \pm 0.096	0.299 \pm 0.056	0.177 \pm 0.098	0.335 \pm 0.145	0.422 \pm 0.106	0.424 \pm 0.107	0.429 \pm 0.109
nmes	0.060 \pm 0.122	-0.049 \pm 0.268	-0.068 \pm 0.260	-0.061 \pm 0.208	-0.006 \pm 0.253	0.004 \pm 0.241	0.001 \pm 0.242